Proceedings of ISFOG 2025
5TH INTERNATIONAL SYMPOSIUM ON
FRONTIERS IN OFFSHORE GEOTECHNICS
Nantes, France | June 9-13 2025

ISBN 978-2-85782-758-0

Analyses of spudcan penetration and its effect on an adjacent offshore WTG monopile foundation

V. A. Drosos*, Y. K. Chaloulos, P. Tasiopoulou, P. Georgarakos, A. Giannakou, J. Chacko
GR8 GEO, Athens, Greece

**vdrosos@gr8-geo.com (corresponding author)*

ABSTRACT: This paper presents the numerical evaluations performed to assess the effect of spudcan penetration and extraction adjacent to the monopile foundation (MP) of an offshore WTG. The analyses aimed to estimate changes in stratigraphy, seabed condition, and soil strength due to spudcan installation and extraction, evaluate their impact on monopile lateral capacity, and assess the effectiveness of mitigation measures.
For the assessment of spudcan penetration and extraction and the extent of disturbance, Finite Element analyses were performed. Due to the highly nonlinear nature of the penetration problem, a large deformation formulation was utilized in conjunction with the Coupled Eulerian-Lagrangian (CEL) technique in ABAQUS. The numerical approach adopted was validated against a case-history and a centrifuge test. Significant spudcan penetrations, on the order of 20 meters, were simulated with post-extraction depressions on the order of 2 meters.
For the assessment of the impact of spudcan penetration and extraction on the MP lateral response, 3D pushover analyses were performed with the finite difference code FLAC3D. The numerical analyses were intended to model the nonlinear MP-soil interaction due to the static monotonic application of a load combination at the top of the MP resulting in the development of shear, axial force and bending moment at seafloor level. Analyses results indicated that mitigation measures (filling of the spudcan depression with rock) and the presence of scour protection (which was not considered in the original MP design) provide additional resistance which exceeds the effects of spudcan disturbance.

Keywords: Spudcan; Monopile; Interaction; Penetration; Extraction

1 INTRODUCTION

Offshore wind energy projects are pivotal to achieving global renewable energy goals. However, the geotechnical challenges associated with these projects, particularly in regions with complex soil conditions, demand innovative engineering solutions.

One of the primary challenges during the construction of an offshore wind farm (OWF) was the assessment of the potential impact on the monopiles by the jack-up vessels operation. The observed significant penetration of the spudcans (up to 19 m deep) and the disturbance of the soil in the vicinity of the monopiles raised concerns about the lateral resistance of monopiles, particularly under extreme loading conditions.

This paper describes how the impact of the spudcan-induced soil disturbance on monopile behavior was assessed using advanced numerical simulations. First, Coupled Eulerian-Lagrangian (CEL) techniques were used in ABAQUS to model the spudcan penetration/extraction and to estimate the extent and properties of the disturbed zone. Then, the disturbed zone was introduced to a finite difference model in FLAC3D and 3D pushover analyses were performed to evaluate monopile performance after jack-up vessel installation operations. The study further assesses the effectiveness of scour protection measures in mitigating these effects.

2 SITE CONDITIONS AND STRUCTURES

2.1 Site conditions

The soil layers below seabed at the location studied consist of the following, in descending sequence:

- an ~5m thick medium dense to dense sand layer (Unit I). The interpreted relative density (D_r) of the sand is ~ 70%. An ~1m thick fine-grained clayey interlayer lies between~ 2 and 3 m depth;
- an ~12m thick firm to stiff lean clay layer (Unit II) below Unit I with undrained shear strength (S_u) varying from ~20 to 90 kPa;
- a 7.5m thick stiff to very stiff fat clay layer (Unit III) below Unit II with S_u varying from ~90 to 130 kPa;
- a sequence of medium dense sand layers (Unit IV) below Unit III (>25m depth) with interpreted D_r between 40- and 50%.

The soil properties considered in the analyses are summarized in Table 1.

Table 1. Idealized Soil Properties.

Unit	Top Depth (m)	Unit Weight (kN/m^3)	Relative Density (%)	Undrained Shear Strength (kPa)	Small-strain Shear Modulus (MPa)
I	0	17.5	70		5+6.73z
II	5	17.5		20-87	12-44
III	16.7	18.0		87-132	44-65
IV	24.2	20.0	50		175
V	29.8	20.0	40		175

Rock material was planned to be used around the monopile for scour protection. A schematic of the scour protection is shown in Figure 1.

2.2 Monopile

The MP foundation is a steel pipe with external diameter of 7.8 m and varying wall thickness (from 60 to 86 mm) with depth. The uppermost section of the monopile was extended up to ~12m above sea level to coincide with the load application point. Two scenarios were analyzed (Figure 1): a) including the scour protection, and b) assuming no scour protection.

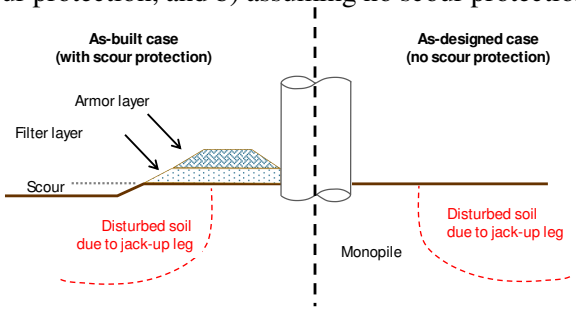

Figure 1. Sketch of cases analyzed: (left) as-built case with scour protection, (right) as-designed case (not to scale)

2.3 Spudcan

The jack-up vessel used for the installation of the monopiles was equipped with four tubular legs each with 14 x 9 m (maximum bearing area, MBA) rectangular spudcans with a tip-to-MBA height of 1 m.

3 ASSESSMENT OF SPUDCAN-INDUCED DISTURBANCE

3.1 Modeling approach

For the assessment of spudcan penetration and extraction and the estimation of the disturbed soil volume, numerical analyses were performed using the Finite Element Method (FEM). A large deformation formulation available in ABAQUS was utilized in conjunction with the CEL technique. This approach has been used by several researchers for the analysis of similar problems (e.g. Hossain et al., 2014). The spudcan is modelled as a rigid Lagrangian body while the soil is discretized using Eulerian elements.

The FE analyses of the spudcan penetration/extraction were performed in two steps:

- Step 1 – Penetration: The spudcan is pushed into the idealized soil profile to simulate the penetration down to the depth measured in the field with a typical penetration rate of 1 m/h. During penetration, the soil resistance is recorded and the penetration depth-load curve is compared with the leg penetration field data acquired during installation.
- Step 2 – Extraction: In this step the spudcan is extracted from the penetration depth reached during Step 1. The disturbed zone is assessed and the final soil properties (i.e. soil type, shear strength) within this area are extracted from the analysis results for use in the monopile model to estimate the effect of disturbance on monopile response.

The FE model developed for the simulation of the spudcan penetration is shown in Figure 2. Only one-quarter sector of the domain was modeled accounting for the inherent symmetry. The soil element size along the trajectory of the spudcan is about 0.025D (where D is the spudcan diameter) following the recommendations of Hu et al. (2015). A frictional contact was defined for the soil–spudcan interaction based on the Coulomb friction model ($\mu = 0.5$).

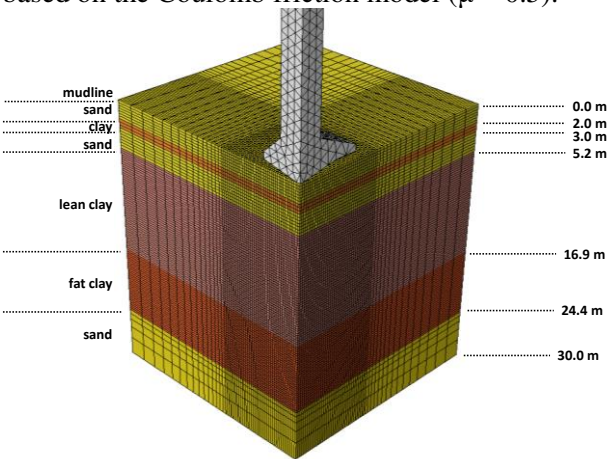

Figure 2. 3D view of the numerical model used for the analysis of the spudcan penetration/extraction

Cohesive soil was modeled as a linear elastic-perfectly plastic material using a Tresca yield criterion, extended to capture strain rate and strain softening effects. Given the relatively fast penetration of the spudcan, undrained conditions were considered. The undrained shear strength of the cohesive soil was modified in every time increment to account for rate effects (typically an increase in strength) and strength degradation using the relationship proposed by Hossain and Randolph (2009). As shown on Figure 3, soil strength reduces with increasing absolute plastic

shear strain from the intact strength to a fully remolded strength.

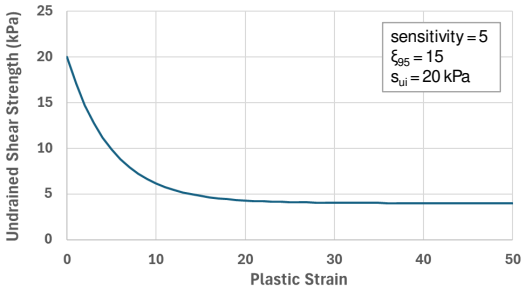

Figure 3. Example of strain-induced strength degradation per Hossain and Randolph (2009)

The nonlinear behavior of the sand was modeled using a modified Mohr-Coulomb law allowing post-peak softening of the friction angle with accumulated plastic strain (Anastasopoulos et al., 2007). A 7% absolute plastic strain threshold was assumed for reaching the critical state friction angle which was assumed to be 33° for both sand layers. A linear degradation function was adopted for the sand.

3.1.1 Modeling approach validation

The numerical approach described above has been validated against a field case and a centrifuge test.

3.1.1.1 Spudcan penetration: case history

A case history of a spudcan installation in the Gulf of Mexico (Menzies and Roper, 2008; Hossain et al., 2014) was used for the validation of the model capability to accurately represent the penetration of a spudcan with similar size to that analyzed in this study.

A spudcan with a diameter of 12.2 m penetrated a clay layer with an undrained shear strength profile increasing from about 15 kPa at the seafloor to about 45 kPa at a depth of 24 m. The penetration resistance of all three legs was measured in the field during installation.

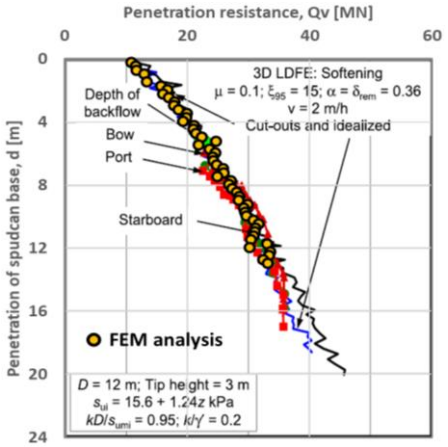

Figure 4. Comparison of FEM predictions (yellow dots) against field measurements (red squares). Numerical analyses results from Hossain et al. (2014) using a similar approach are shown with the black and blue lines

The predictions of the model for this case history are compared to the field measurements in Figure 4. A good agreement has been achieved between predictions, field measurements, and earlier predictions made by Hossain et al. (2014) who analyzed the specific case history with a similar modeling approach.

3.1.1.2 Spudcan penetration and extraction: centrifuge test

Centrifuge tests conducted and reported by Kohan et al. (2014) were analyzed with the developed numerical model to validate its ability to capture the phenomena during spudcan extraction.

In this centrifuge test series, a 6-m (prototype scale) diameter spudcan was pushed into a soft clay layer ($s_u \approx 1$ to 22 kPa at 20m depth) to an installation depth of 9 m and after some idle time the spudcan was pulled up until complete extraction from the soil. The idle time that represented the operation period varied from zero to three years (in prototype scale) and thus the effect of the duration of the operation time on spudcan extraction was investigated.

The numerical approach described above was used to analyze two tests from the experimental series: a) the immediate extraction (zero operation period), and b) a long operation period (i.e. 3 years) during which the near normally consolidated soil is assumed to regain its initial strength due to reconsolidation. The FEM predictions of penetration and extraction resistance are compared to the experimental data in Figure 5 for the two cases analyzed. In general, the numerical model captures reasonably the performance of the spudcan during both penetration and extraction.

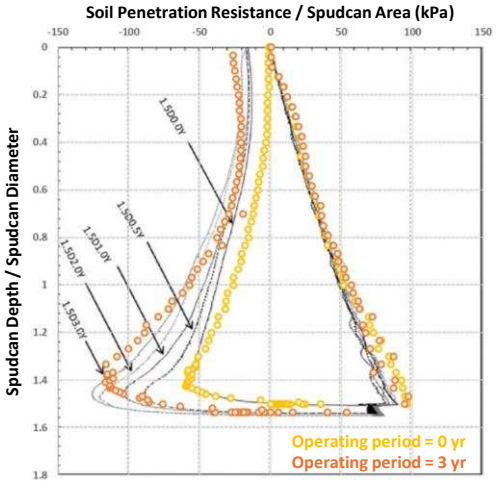

Figure 5. Comparison of FEM predictions (circles) and experimental data (lines) for the analyzed centrifuge test

3.2 Spudcan penetration/extraction analyses

The results of the spudcan penetration analyses for the case described in Section 2 are presented in Figure 6

to Figure 9. Figure 6 shows the deformed soil domain for a penetration depth of 20 m and contours of soil plastic strains which reveal the extent of disturbance. In the same figure the topology of the surficial sand layer is presented. At the surface the characteristic soil depression created by spudcan installation is observed. Under the spudcan, a block of soil with reduced plastic strains is discerned on Figure 6a. This block is a sand plug pushed by the spudcan through the softer clay layers as the spudcan penetrates the soil (Figure 6b).

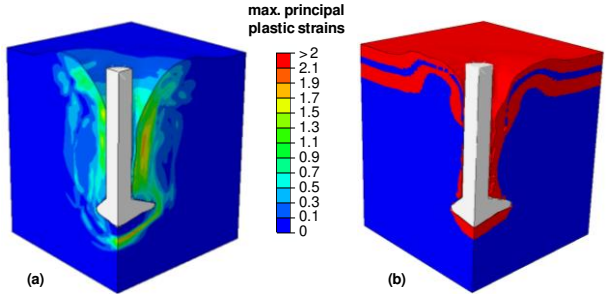

Figure 6. (a) Deformed soil domain and contours of maximum principal plastic strains for 20 m penetration depth; (b) Topology of the surficial sandy material. The displaced sand plug and the sand backflow are discerned

The FEM results in terms of the required force to penetrate the spudcan are compared on Figure 7 with the approximate range of field measured applied loads per leg during installation. Significant differences were observed in the penetration resistance between the four legs of the jack-up. The differences can perhaps be attributed to variability in soil conditions between leg locations, and/or to differences in operations during penetration (cycling during penetration, jetting, etc.). The FE analyses results agree reasonably well with the measurement range, especially for penetration depths greater than 3.5 m, both in terms of penetration depth under preload and penetration resistance increase with depth. It is noted that there are still stratigraphic and material property idealizations and in some cases cycles of loading/withdrawal (with jetting) used during the installation sequence which are not modeled in these analyses. The underestimation of the penetration resistance in the first 4 m could perhaps in part be attributed to a stronger top sand layer that was not modelled (adjacent boreholes showed for example a shallow cemented layer). Menzies and Roper (2008) show 25% variations between legs during a given installation as well and indicate that similar or greater variations between observed and predicted resistances are not uncommon.

Subsequently spudcan penetration, extraction was simulated. In this step, the spudcan was extracted from a penetration depth of about 20 m. The goal of this analysis was to assess volume of disturbance after spudcan extraction and estimate post-extraction soil properties (i.e. soil type, shear strength) in this zone. The information obtained from the extraction analysis was then used in a monopile model to estimate the effect of the spudcan penetration/extraction on the lateral response of the foundation. It is noted that jetting which facilitates the extraction of the spudcan was not modeled in these analyses.

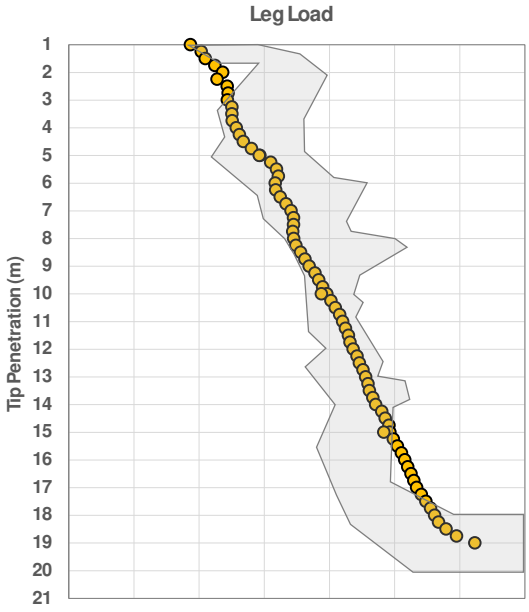

Figure 7. Comparison of analysis results (circles) with approximate range of applied loads per leg (shaded area)

The extent of the disturbed zone is shown in Figure 8 in plan and section views. Close to the surface the disturbed zone extends roughly one spudcan diameter from the leg axis, while deeper (i.e. below 5 m depth) its extent reduces to about 3/4 of the spudcan diameter. The size of the disturbed soil area is in accordance with the values usually observed (ABS, 2017).

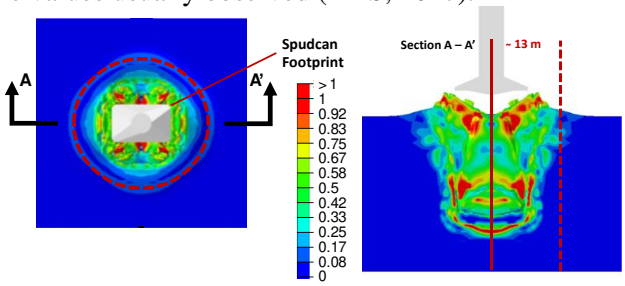

Figure 8. Maximum principal plastic strain contours indicating the disturbed soil area extent after extraction

Figure 9 shows S_u in the clay-dominant soils (Unit II and III) following the collapse of the spudcan sidewalls. As shown, most of the soils in the sheared zone are near residual strength. The actual value of the residual strength varies with depth since the materials are moved around by the spudcan during penetration and extraction.

Following extraction, the material types and associated strengths were extracted and used as inputs for the monopile analyses as described below.

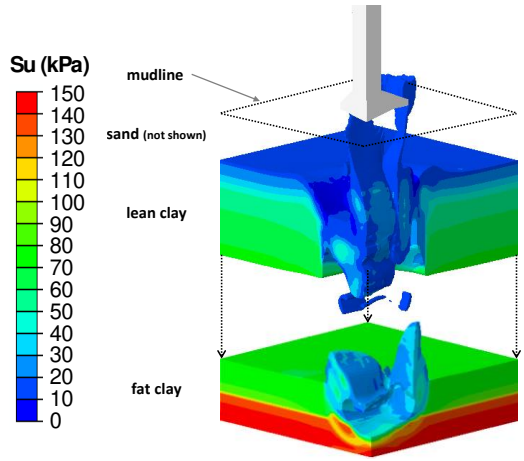

Figure 9. Snapshot of undrained shear strength in the clay units following spudcan extraction and hole collapse

4 IMPACT ON MONOPILE RESPONSE

4.1 Modeling approach

To evaluate the impact of spudcan penetration and extraction on the MP lateral response, 3D numerical analyses were performed with FLAC3D. The numerical analyses were intended to model nonlinear MP-soil interaction under static monotonic (pushover) application of a load combination at the top of the MP.

The MP pushover analyses were performed in three steps. First, gravity loads were applied, and the model was brought to equilibrium. Subsequently, the axial load was applied at the top of the MP and the model was brought to equilibrium. In the last step a horizontal displacement is applied at the top of the MP (resulting in shear force and bending moment at seafloor level). Details on the modeling approach followed for MP lateral analyses and validation of the methodology are given in Tasiopoulou et al. (2020;2025).

Monopile lateral response analyses were performed for the as-designed case (i.e., no disturbance from the spudcan penetration) as well as for the as-built case (i.e., considering the disturbance from the spudcan) and the responses were compared to each other. The model developed for the as-built case is shown in Figure 10. For the as-built case, the strength and stiffness degradation resulting from the spudcan installation and extraction process were introduced in the FLAC3D model. The mesh around the spudcan location was densified to better capture the resulting variation in stratigraphy/properties. Figure 11a illustrates the variation of S_u (cohesion) within the clay layers. The clay soils most affected by the spudcan which have residual strengths are shaded blue while the lighter blue colors show reduced clay strengths (but higher than residual). Similarly, Figure 11b presents friction angle variations within the sand layers. The residual friction angle is shown in blue. As shown on this figure the sand plug below the spudcan maximum penetration depth and most of the surficial sand layer (Unit I) between the spudcan and the MP have reached their residual (critical state) strength.

The nonlinear behavior of the scour protection layers was modeled using the Itasca S3 model in FLAC3D assuming $\varphi = 45^o$ and $\varphi = 42^o$ for the armor and the filter layer, respectively.

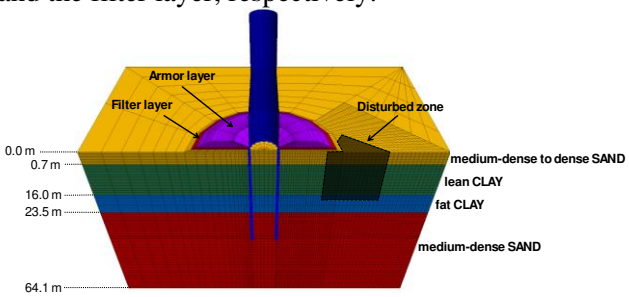

Figure 10. 3D Finite difference mesh of as built case

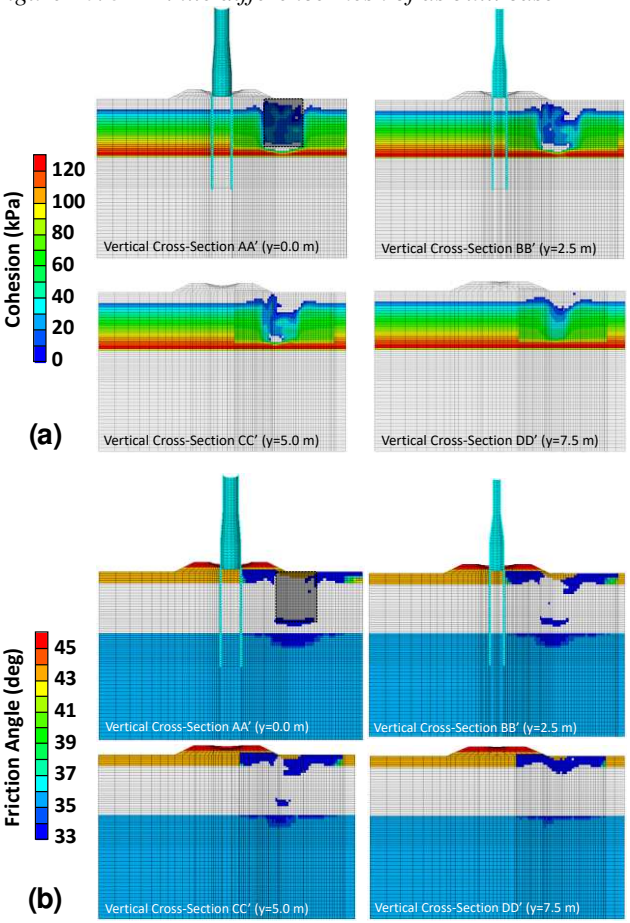

Figure 11. Variation of strength properties on different cross-sections in the out-of-plane direction: (top) undrained shear strength within the clay layers; (bottom) friction angle within the sand layers

Additional 3D numerical MP pushover analyses were performed to evaluate the relative effects of scour protection on MP lateral response.

4.2 MP lateral response analyses

The results of the numerical evaluations for the cases analyzed are shown on Figure 12 in terms of

normalized (to the as-designed capacity) lateral load versus displacement at seabed level. The as-designed case (Case 1 – original strength; no scour protection) response is shown with the black line. The results for the as-built cases considering no scour protection are shown with the blue and yellow lines for undisturbed (Case 2) and disturbed (Case 3) soil conditions respectively. Finally, analyses results for the as-built cases including scour protection are shown with the red and green lines for undisturbed (Case 4) and disturbed (Case 5) soil conditions respectively.

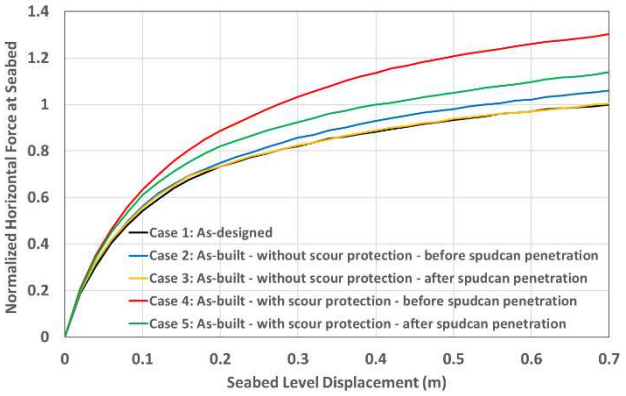

Figure 12. Lateral load vs horizontal displacement MP response at seabed level for all cases analyzed

Cases 2 and 3 (without scour protection) are close to the design case (Case 1). The effect of soil disturbance is typically more apparent at large displacements (above those corresponding to the approximate ULS load level), most likely because the disturbed zone is in the order of 15 meters from the monopile and some displacement is required to mobilize resistance from this zone. We note that the slightly higher loads after 0.25m of seabed displacement observed for Case 2 compared to Case 1 are likely due to small differences between the two cases (different lever arms; small differences in the monopile geometry and penetration due to scour) as well as differences in mesh discretization where a finer mesh has been introduced in Cases 2 and 3 (i.e. the displacements at which different parts of the mesh are engaged may introduce a small discontinuity).

The stiffening effect of incorporating the scour protection is demonstrated in Cases 4 and 5. The beneficial effect of the scour protection exceeds the detrimental effect of soil disturbance.

5 CONCLUSIONS

Advanced numerical methods were used to assess the possible impact of deep spudcan penetration on the lateral response of a WTG monopile. Large deformation analyses using the CEL method in ABAQUS were used to assess the extent of the disturbed soil zone and the associated impact on soil properties. The results were extracted and used as input in a nonlinear analysis of the lateral performance of the monopile in FLAC3D.

The analyses showed that for this case the potential temporary reduction of the monopile stiffness in the lateral direction due to soil disturbance is small and can be counterbalanced, at least temporarily, by considering the additional lateral resistance from the scour protection layer installed around the MP.

AUTHOR CONTRIBUTION STATEMENT

All Authors: Conceptualization, Methodology, Formal Analysis, Writing-Original draft, Writing-Review and Editing.

REFERENCES

ABS – American Bureau of Shipping (2017) Geo-technical Performance of Spudcan Foundations, Guidance Notes (updated March 2018)

Hossain, M. S., and Randolph, M. F. (2009) Effect of strain rate and strain softening on the penetration resistance of spudcan foundations on clay, International Journal of Geomechanics, 9(3), pp. 122–132

Hossain, M. S., Zheng, J., Menzies, D., Meyer, L. & Randolph, M. F. (2014) Spudcan penetration analysis for case histories in clay, Journal of Geotechnical and Geoenvironmental Engineering, ASCE, 140(7), pp. 04014034-1– 04014034-13

Hu, P., Wang, D., Stanier, S. A., and Cassidy, M. J. (2015) Assessing the punch-through hazard of a spudcan on sand overlying clay, Geotechnique, 65(11), pp. 883–896

Kohan, O., Gaudin, C., Cassidy, M.J., and Bienen, B. (2014) Spudcan extraction from deep embedment in soft clay, Applied Ocean Research, Elsevier, 48, pp. 126-136

Menzies, D., and Roper, R. (2008) Comparison of jackup rig spudcan penetration methods in clay, In: Proceedings of Offshore Technology Conference, Houston, USA

Tasiopoulou P., Chacko J., Chaloulos Y., Giannakou A., and Gerolymos N. (2020) Insight into the cyclic response of OWT pile foundations in sand: Numerical simulation of PISA field tests, Proceedings of 4th International Symposium on Frontiers in Offshore Geotechnics, Austin, USA, August 16-19

Tasiopoulou, P., Limnaiou, T., Giannakou, A., and Chacko, J. (2025) "Insight into the cyclic response of OWT pile foundations in clay: Numerical simulation of PISA field tests", Proceedings of 5th International Symposium on Frontiers in Offshore Geotechnics, Nantes, France, June 9-13